

1
2
3
4
5
6

7
8
9
10
11
12
13
14
15
16
17
18
19

20

21
22
23
24
25

26

27

Supporting Information *for*

Haze episodes before and during the COVID-19 shutdown in Tianjin, China: Contribution of fireworks and residential burning

Qili Dai^{1,2}, Jing Ding^{2,3}, Linlu Hou^{1,2}, Linxuan Li^{1,2}, Ziyang Cai³, Baoshuang Liu^{1,2},
Congbo Song⁴, Xiaohui Bi^{1,2}, Jianhui Wu^{1,2}, Yufen Zhang^{1,2,*}, Yinchang Feng^{1,2}, Philip
K. Hopke^{5,6}

1. State Environmental Protection Key Laboratory of Urban Ambient Air Particulate
Matter Pollution Prevention and Control, College of Environmental Science and
Engineering, Nankai University, Tianjin 300350, China

2. CMA-NKU Cooperative Laboratory for Atmospheric Environment-Health Research
(CLAER), College of Environmental Science and Engineering, Nankai University,
Tianjin 300350, China

3. Tianjin Environmental Meteorological Center, Tianjin 300074, China

4. School of Geography Earth and Environment Sciences, University of Birmingham,
Birmingham B15 2TT, UK

5. Department of Public Health Sciences, University of Rochester School of Medicine
and Dentistry, Rochester, NY 14642 USA

6. Institute for a Sustainable Environment, Clarkson University, Potsdam, NY 13699
USA

Contents of this file

Text S1 to S2

Figures S1 to S9

Tables S1 to S2

* Author to whom correspondences should be addressed. Email: zhafox@nankai.edu.cn (Y. Zhang), Tel.: +862223503397; Fax: +862223503397

28 **Text S1. HYSPLIT backward-trajectory calculation.**

29 Air trajectory analysis provides useful information regarding the spatial scale of
30 the airflows that arrived at a given location (here N 38.99°, E 117.34°). 48 h backward
31 trajectories were calculated at heights of 100 m AGL using the Hybrid Single-Particle
32 Lagrangian Integrated Trajectory (HYSPLIT) for every hour during the measurement
33 campaign. Clustering analysis was performed for the derived 48 h backward trajectories
34 thus produced four clusters: C1-Southwestly, C2-Northerly, C3-Northeasterly, and C4-
35 Northwesterly (Fig. S6).

36

37 **Text S2. Evolution of pollution episodes**

38 *HE1.* The peak values of PM_{2.5} in the studied cities were decreased from the north
39 (Beijing) to the south (Cangzhou) of the BTH region. Before reached its peak value at
40 11:00 on 4 January (Fig. 1a), the PM_{2.5} concentration in Tianjin elevated under poor
41 dispersion conditions that associated with low VC values (Fig. 2(b, c, d)), periods of MLH
42 less than 400 m and weak surface winds, resulting in average hourly increase rate of 2 μg
43 m⁻³ PM_{2.5} per hour. Surface winds in Tianjin were gradually shifted from SW-W to N at
44 heights below 3 km AGL (Fig. 1(c, d)). Since then, the pollutants were carried off by cold
45 high-speed N and NE winds (Fig. 2b). Given that the arrival time of the N winds to each
46 city delayed from north to south in the BTH region, the pollution episode was first ended
47 in Beijing, followed by Lang'fang, Tangshan, Tianjin and Cangzhou (Fig. 1a). The end of
48 HE1 in Tianjin was facilitated by the sharply increased VC (>1000 m² s⁻¹) in the late
49 afternoon on 4 January.

50 *HE2.* There were four transient periods with pronounced increases in PM_{2.5} during
51 HE2. The PM_{2.5} concentration was sharply elevated from ~ 50 μg m⁻³ to the first peak
52 value of 175 μg m⁻³ when the air masses started shifting from N to SW in the early
53 morning (05:00) on 15 January, together with MLH remained <200 m and surface wind
54 speed as weak as <1 m s⁻¹. During this period enhanced by poor dispersion, the average
55 increase rate of PM_{2.5} was 18.3 μg m⁻³ h⁻¹, with a maximum rate of 29 μg m⁻³ PM_{2.5} per
56 hour. The first peak value in Tianjin was higher than other mentioned surrounding cities.
57 There was significantly elevated number concentration of particles with sizes around 100
58 nm without notable size shifting in the morning on 15 January (HE2), which was likely

59 resulted from near-surface regional transport. The second pronounced increase of PM_{2.5}
60 from 127 $\mu\text{g m}^{-3}$ to the second peak value of 285 $\mu\text{g m}^{-3}$ was due to the decrease of MLH
61 from ~ 700 m to ~ 200 m, as well as wind speed decreased from 1.5 m s^{-1} to less than 1 m
62 s^{-1} . The average increase rate of PM_{2.5} was $9.2 \mu\text{g m}^{-3} \text{ h}^{-1}$, with a maximum rate of $42 \mu\text{g}$
63 $\text{m}^{-3} \text{ PM}_{2.5}$ per hour. In the afternoon of 16 January, a weak humid northerly wind arrived
64 at Tianjin for a short period thus reduced the surface PM_{2.5} concentrations. The third
65 shapely increase of PM_{2.5} from 156 to 285 $\mu\text{g m}^{-3}$ was again partly due to the decrease of
66 MLH, with a maximum increase rate of $22 \mu\text{g m}^{-3} \text{ h}^{-1}$. From the night of 17 January to the
67 next day, it was foggy with rime appeared on a large scale. Note that a persistent strong
68 temperature inversion above the fog (>200 m AGL) was observed in the early morning of
69 18 January. The low temperature and high humidity within the MLH provided favorable
70 conditions for the formation of sulfate and nitrate through aqueous-phase and/or
71 heterogenous chemistry. Those adverse meteorological effects together resulted in the
72 fourth elevation of PM_{2.5} from 113 to 293 $\mu\text{g m}^{-3}$ within 10 h, with an average increase
73 rate of PM_{2.5} of $20 \mu\text{g m}^{-3} \text{ h}^{-1}$ (maximum value of $48 \mu\text{g m}^{-3} \text{ h}^{-1}$). Since then, the PM_{2.5}
74 was gradually decreased along with the surface winds increased to $\sim 2 \text{ m s}^{-1}$. With the
75 arrived air masses shifted from SW ($2\sim 3 \text{ m s}^{-1}$) to N to NW ($\sim 16 \text{ m s}^{-1}$), PM_{2.5} quickly
76 declined from ~ 173 to $\sim 20 \mu\text{g m}^{-3}$. As shown in Fig. 1b, the end of HE2 in Beijing ahead
77 of those in Langfang, Tangshan, Tianjin and Cangzhou. Overall, the three times drop of
78 PM_{2.5} in HE2 were all occurred during daytime when MLH rose. Whereas every shapely
79 increases of ground PM_{2.5} associated with decreased MLH at nighttime as a likely result
80 of the downmixing of aerosol aloft (Fig. 1b), particularly for the last increase. In that
81 case, the increase of PM_{2.5} in Tianjin was ahead of those in Langfang, Beijing and
82 Tangshan, suggesting the pollution transported from south to north of the BTH.

83 *HE3.* The PM_{2.5} concentrations were elevated to pollution level ($>75 \mu\text{g m}^{-3}$) at
84 the late night of 21 January when the air masses shifted from N to SW with speed
85 decreased from $>10 \text{ m s}^{-1}$ to $<2 \text{ m s}^{-1}$, concurrent with MLH decreased from ~ 800 m to
86 <200 m. The PM_{2.5} concentrations increased again around next midday, during the time
87 when MLH and surface wind speed rose. Meanwhile, there was clearly sinking of aerosol
88 at late night of 21 January (Fig. 3). Before PM_{2.5} reached its maximum value, the MLHs
89 were stay below 200 m, surface wind speeds were $<1.0 \text{ m s}^{-1}$, and the average air masses

90 speed approximate 1.5 m s^{-1} . In this stagnant environment, the ground temperature was
91 below 0°C and RH reached about 90%. $\text{PM}_{2.5}$ gradually increased to the maximum value
92 ($239 \mu\text{g m}^{-3}$) from the afternoon of 22 January to the next morning, accompanied by
93 strong sinking of aerosol from $>1.0 \text{ km AGL}$ down to the ground (Fig. 1b). Since then,
94 $\text{PM}_{2.5}$ concentrations were declined to $89 \mu\text{g m}^{-3}$ then increased again to $113 \mu\text{g m}^{-3}$, as
95 the MLH elevated from 150 to 1000 m and surface winds increased from ~ 1.0 to $\sim 5.0 \text{ m}$
96 s^{-1} . The last increase of $\text{PM}_{2.5}$ was possibly caused by winds convergence in Tianjin. The
97 SE winds run into the N winds for a short period (Fig. 1(c, d)). Pollutants were
98 aggregated in Tianjin before the strong dry northerly winds arrived at 19:00 on 23
99 January with moving speeds great than 13.0 m s^{-1} . The wind profiler radar also observed
100 strong convection flows after the MLH increased (Fig. 1b). The last increase of PM
101 before the end of the pollution episode was featured enhanced particle number
102 concentrations as shown in Fig. 3d, which was caused by regional transport since the
103 airflows were able to carry pollutants from upwind polluted areas, thus exacerbating local
104 pollution. It should be noted that the northerly airflows have passed through Tangshan
105 before arrival in Tianjin (Fig. 2b). Fig. 1a also clearly demonstrates that HE3 was ended
106 first in Beijing, then in Langfang, Tangshan and Tianjin, and Cangzou. The shape of
107 $\text{PM}_{2.5}$ concentrations of HE3 is more similar to HE1 than other HEs.

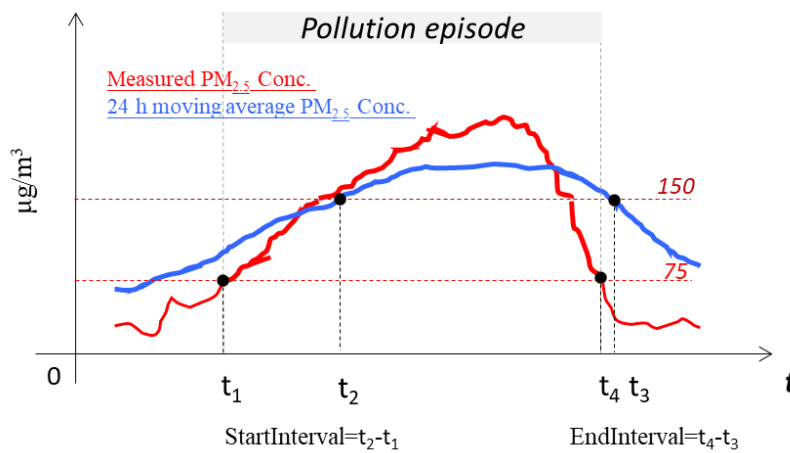
108 *HE4*. HE4 was gradually formed since the midnight of 24 January (Chinese New
109 Year Eve) when the direction of air masses shifted from N-NE to SW. The speeds of air
110 masses were decreased from ~ 10 to $3\sim 4 \text{ m s}^{-1}$ and the MLH remained $<200 \text{ m}$ until $\text{PM}_{2.5}$
111 reached to its highest value of $280 \mu\text{g m}^{-3}$ at 15:00 on 26 January, with average hourly
112 increase rate of $7.0 \mu\text{g m}^{-3} \text{ h}^{-1}$. The fireworks tracer species (SO_2 , Cl^- , K^+ and Mg^{2+})
113 concurrently rose with $\text{PM}_{2.5}$ while NO_2 and CO unchanged. The above results suggest
114 that the increase of $\text{PM}_{2.5}$ may be primarily from fireworks emissions. Fireworks display
115 is a traditional event over China to celebrate the Chinese New Year since a long time ago.
116 Note that fireworks displays were banned throughout Tianjin but this was not the case for
117 other cities in the BTH area particularly in the suburban/rural areas, where fireworks
118 were extensively used. Before $\text{PM}_{2.5}$ reached its peak value, and the air masses were
119 shifted from SW to NE with speed of $\sim 3.0\text{-}4.0 \text{ m s}^{-1}$, and the northeasterly surface winds
120 also increased. Thus, the fireworks emissions were transported from the rural areas

121 surrounding Tianjin, particularly from the northeast of Tianjin where the severest
122 pollution occurred, as shown in the pollution map (Fig. S4). PM_{2.5} was shapely decreased
123 in Tangshan and elevated in Tianjin and Cangzhou (Fig. 1a). During the midnight of 27
124 January, the air masses were shift to SW again for a short period. Since then, PM_{2.5} fell
125 from 265 to 181 $\mu\text{g m}^{-3}$, with an average decrease rate of 9 $\mu\text{g m}^{-3} \text{h}^{-1}$. The last increase
126 of PM_{2.5} in the morning of 29 January was likely due to the downmixing of transported
127 aerosol aloft when the MLH began to rise (Fig. 1b). Though the VC were extremely low
128 during the period of HE4, both the northeast of China and the whole BTH areas
129 experienced serious heavy haze pollution after the Chinese New Year Eve. HE4 was
130 ended by the strong northerly winds that passed through Tangshan, which is similar to
131 HE3. During the daytime of 25 and 26, January, the mass concentrations of both PM₁ and
132 PM_{2.5} transiently increased as the increases of particle number concentration (100-200
133 nm). The sink of regional transport aerosol was responsible for such increases in PM, as
134 confirmed by the aerosol lidar measurement (Fig. 3). In the subsequent developing stage,
135 strong sinking airflows have been frequently recorded (Fig. 1b). The elevated surface
136 secondary inorganic aerosol (SIA) was partly attributed to the sinking airflows.

137 *HE5.* The whole period of HE5 was consisted of two coterminous stages. HE5
138 was formed when air masses shifted from NE and SW, coupled with decreased MLH.
139 During the first stage, PM_{2.5} was increased from ~20 to 171 $\mu\text{g m}^{-3}$ within 42 h, with a
140 average increase rate of 3.5 $\mu\text{g m}^{-3} \text{h}^{-1}$. As is obviously shown in Fig. 1(a, c, d), the
141 shortly alleviation of PM_{2.5} pollution on 8 February was due to the arrival of relatively
142 clean northerly air. From the midnight of 6 February to the early morning of 8 February,
143 the mass concentrations of both PM₁ and PM_{2.5} transiently increased along with the
144 increase of particle number concentration (100-200 nm). The increase in particulate mass
145 concentrations was caused by the sinking of aerosols transported from the southwest (Fig.
146 2b), as confirmed by the aerosol lidar measurement (Fig. 3). Before PM_{2.5} reached its first
147 peak value, a short period of inversion was formed in the morning due to the arrival of
148 the dry and relatively warmer northerly winds in the urban canopy layer (Fig. 1(e, f)).
149 Given that the northerly winds were not strong enough to sweep away all pollutants, the
150 local dispersion condition has backed to stagnant again after it disappeared. After the air
151 masses shifted to SW again, the second stage was formed. During this period,

152 temperature inversion has been observed again and lasted for several days, with the
 153 maximum intensity of $>4^{\circ}\text{C}$ though the ground temperature dramatically rose (Fig. 1f).
 154 The increase of $\text{PM}_{2.5}$ after the midnight of 8 February was associated with elevated K^+ ,
 155 Cl^- and SO_4^{2-} , indicating enhanced emissions from fireworks because it is also popular to
 156 play fireworks during the Lantern festival as well. Winds from SW tend to move
 157 pollutants toward north as $\text{PM}_{2.5}$ in Cangzhou and Tianjin were gradually decreased and
 158 elevated in Langfang and Cangzhou (Fig. 1a). The impact of transported firework-related
 159 emissions on HE5 was likely less strong than that in HE4. The pollutants were finally
 160 removed by the strong northeasterly winds initially originated from the north.

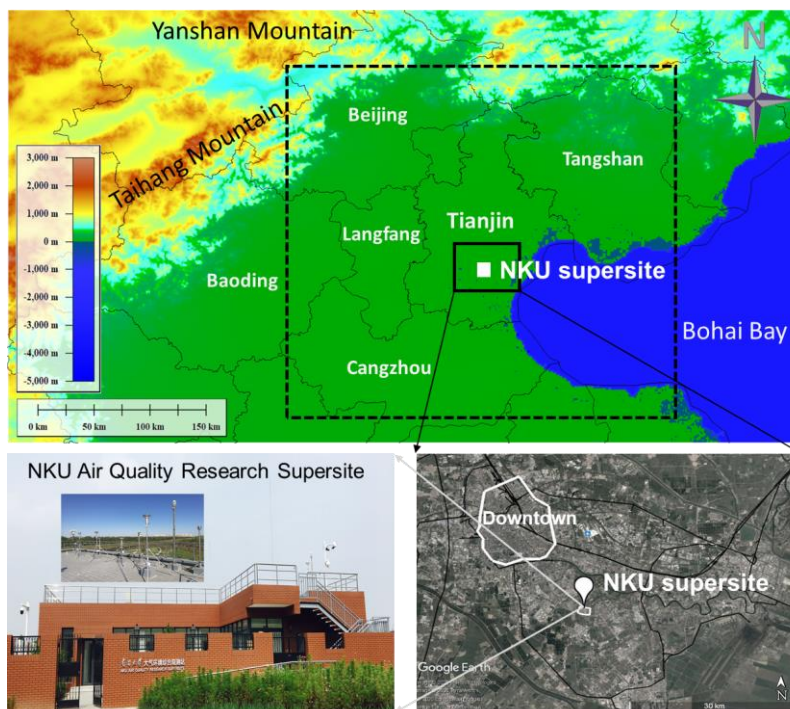
161
 162
 163
 164
 165



166

167 **Figure S1.** Schematic diagram of starting and ending nodes and duration of haze pollution
 168 process. The starting time t_1 is the time when $\text{PM}_{2.5}$ concentration begins to reach $75 \mu\text{g m}^{-3}$,
 169 while the ending time t_4 is the time when $\text{PM}_{2.5}$ concentration begins to decrease below $75 \mu\text{g m}^{-3}$.
 170 The duration is $t_4 - t_1$. This definition was revised based on Zheng et al. (2016).

171
 172

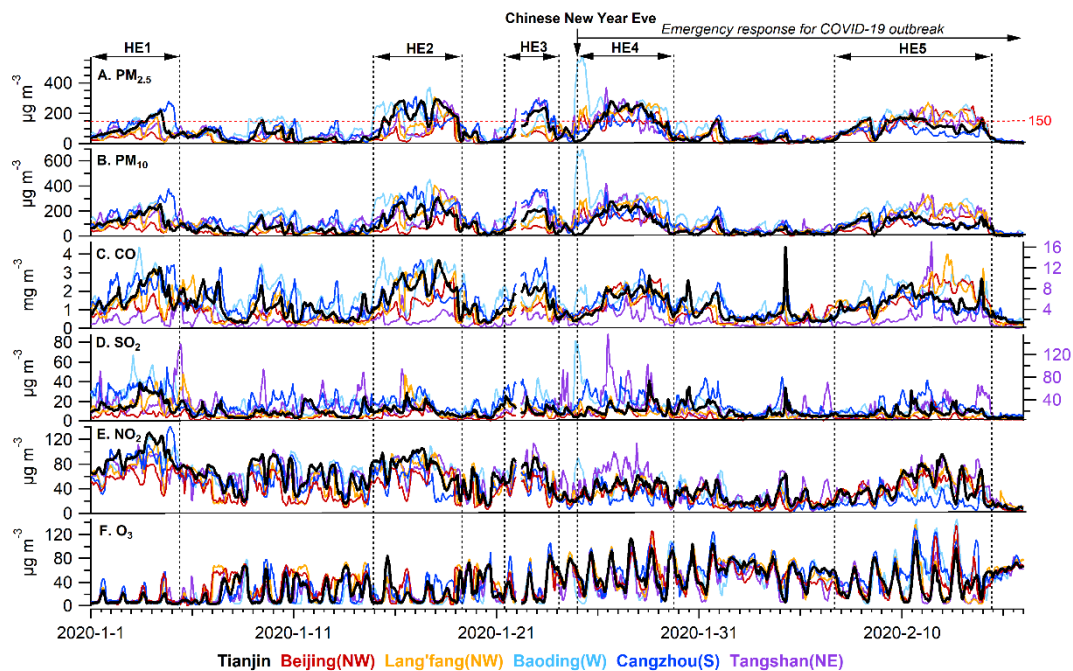


173

174

175

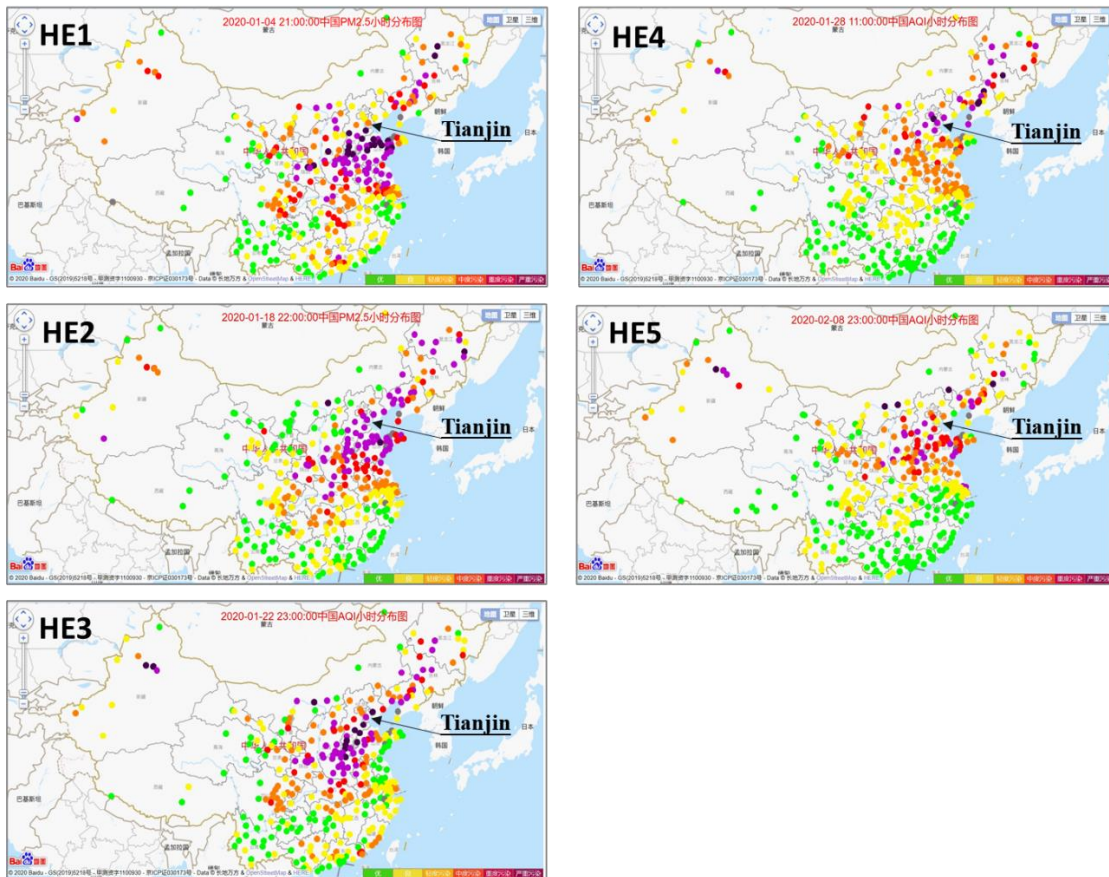
Figure S2. Location of the measurement site in Tianjin.



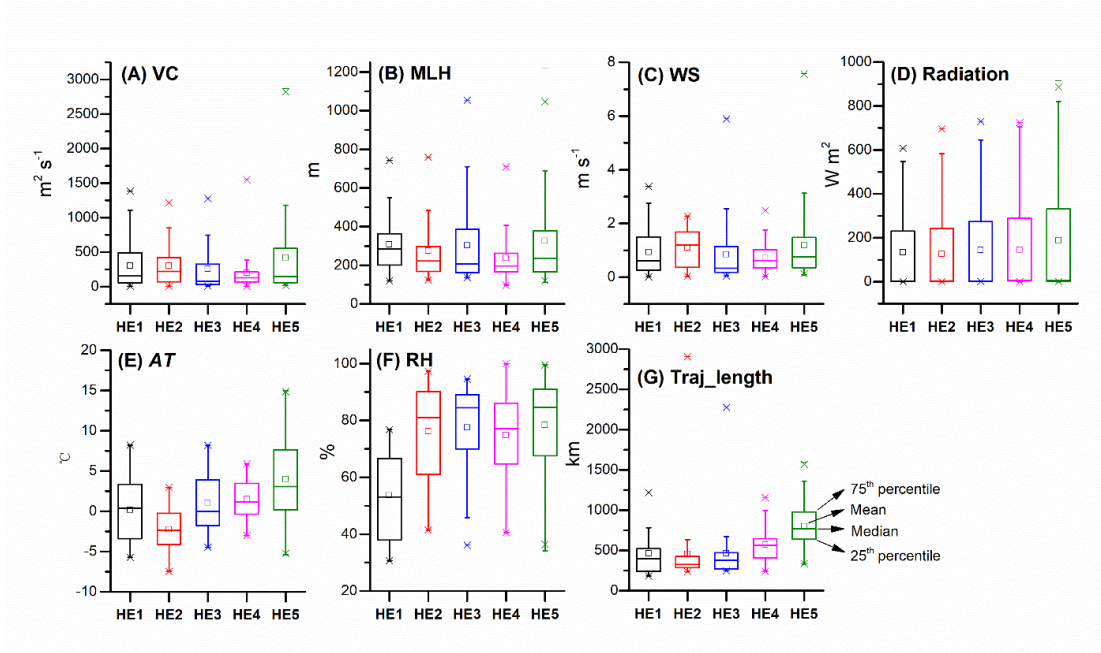
176

177 **Figure S3.** Time series of hourly averaged PM_{2.5}, PM₁₀, CO, SO₂, NO₂ and O₃ concentrations in
 178 Beijing, Tianjin, Lang'fang, Baoding, Tangshan and Cangzhou during the measurement

179 campaign. Beijing and Lang'fang are located at the northwest direction of Tianjin, while
180 Baoding, Tangshan and Cangzhou are seated at west, northeast and south of Tianjin.
181



182
183 **Figure S4.** Screenshots of each HE reaching its maximum spatial scales (Data source:
184 <https://www.aqistudy.cn/>).



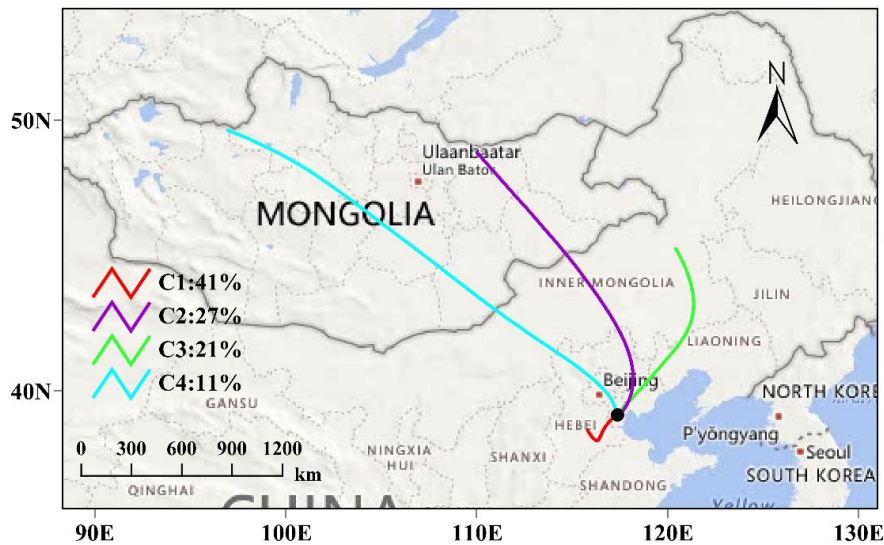
185

186

Figure S5. Boxplots for VC, MLH, WS, radiation, temperature, RH and the length of air mass backward trajectory during each HE.

187

188



189

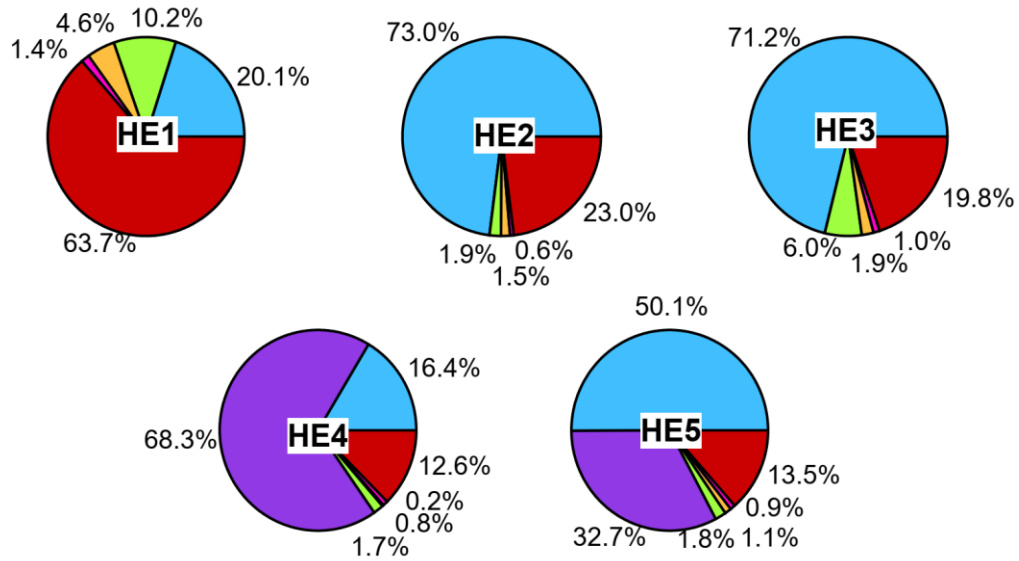
190

Figure S6. Clusters of the 48h air mass backward trajectories arrived in Tianjin at the height of 100 m AGL during the measurement campaign (C1: Southwesterly, C2: Northerly, C3: Northeasterly, C4: Northwesterly).

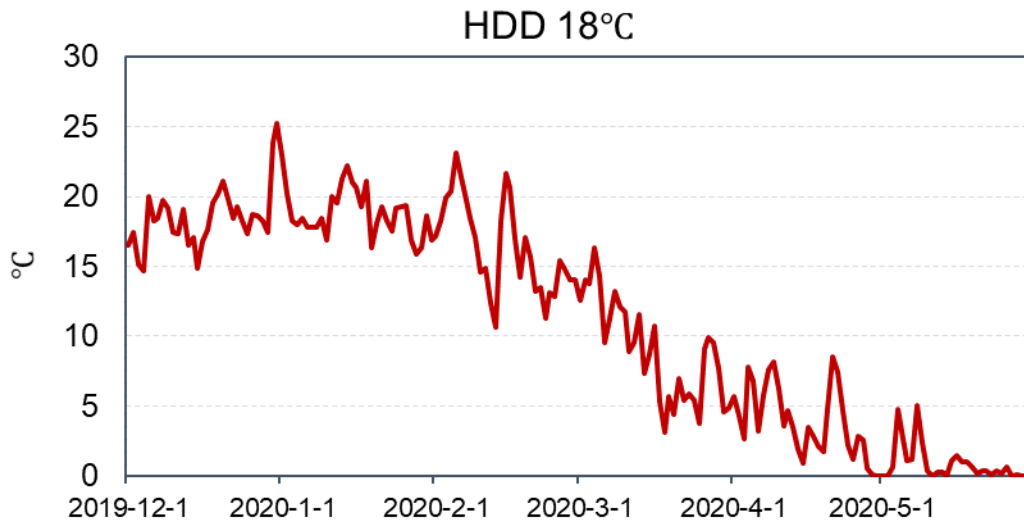
191

192

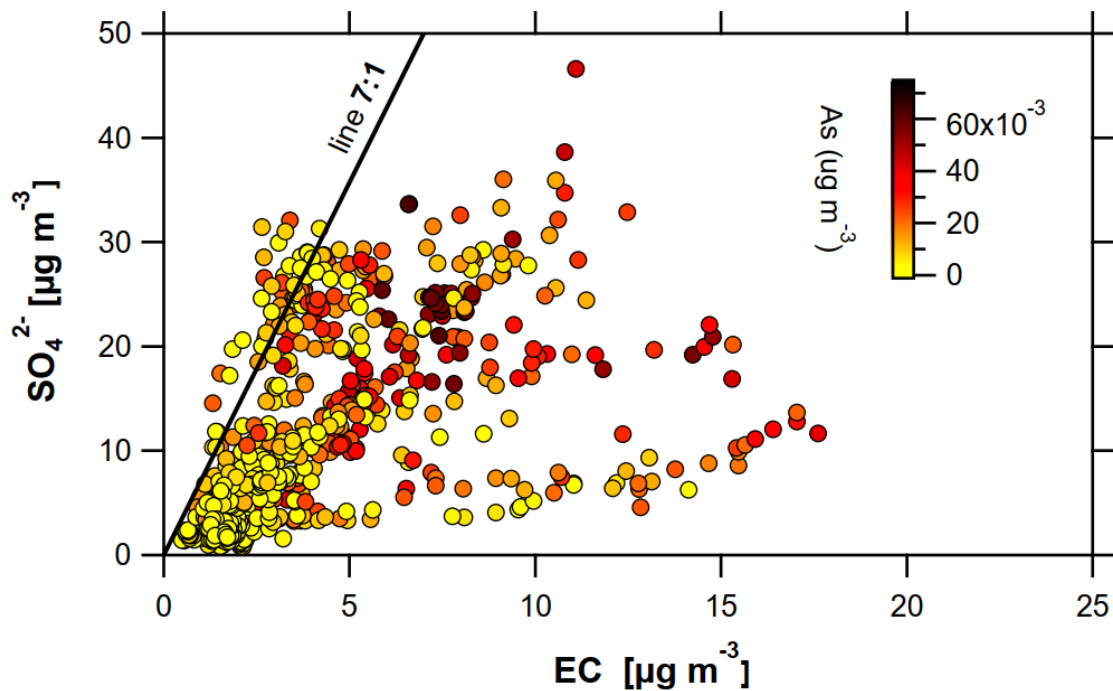
193



194
195 **Figure S7.** Average source contributions to PM_{2.5} during each HE.
196
197



198
199 **Figure S8.** Celsius-based heating degree days with a base temperature of 18°C from December
200 2019 to May 2020 in Tianjin. Data source: www.degree-days.net.
201
202



203

204 **Figure S9.** Scatter plot of SO_4^{2-} versus EC measured during the sampling campaign. Data points
205 were colored by arsenic concentrations. Dash line denotes the 95th percentile line for the ratios of
206 SO_4^{2-} to EC.

207 **Table S1.** Duration and the maximum hourly PM_{2.5} concentrations of the five HEs in Tianjin and
 208 surrounding cities.

	Event	Tianjin	Beijing	Tangshan	Lang'fang	Cangzhou	Baoding
Duration (hr)	HE1	73	-	-	-	75	63
	HE2	93	27	42	81	102	88
	HE3	48	-	49	-	51	41
	HE4	88	89	89	89	85	89
	HE5	174	130	126	129	-	171
Maximum PM _{2.5} ($\mu\text{g m}^{-3}$)	HE1	217	-	-	-	279	202
	HE2	293	234	286	310	311	373
	HE3	239	-	303	-	289	198
	HE4	280	210	370	270	263	571
	HE5	199	249	256	272	-	261

209

210

211 **Table S2.** Squared Person correlation coefficient (r^2) of PM_{2.5} versus primary gaseous pollutants
 212 measured in Tianjin during the five HEs.

	SO₂	NO₂	CO	PM₁₀
E1	0.68	0.77	0.89	0.84
E2	0.00	0.18	0.87	0.89
E3	0.00	0.47	0.65	0.91
E4	0.01	0.09	0.43	0.85
E5	0.01	0.21	0.68	0.89

213